

Structural basis for the diversity of the mechanism of nucleotide hydrolysis by the aminoglycoside-2''-phosphotransferases

Clyde A. Smith,^{a,b*} Marta Toth,^c Nichole K. Stewart,^c Lauren Maltz^a and Sergei B. Vakulenko^{c*}

^aStanford Synchrotron Radiation Lightsource, SLAC National Accelerator Laboratory, Menlo Park, CA 94025, USA,

^bDepartment of Chemistry, Stanford University, Stanford, CA 94305, USA, and ^cDepartment of Chemistry and Biochemistry, University of Notre Dame, Notre Dame, IN 46556, USA. *Correspondence e-mail:

csmith@slac.stanford.edu, svakulen@nd.edu

Edited by R. McKenna, University of Florida, USA

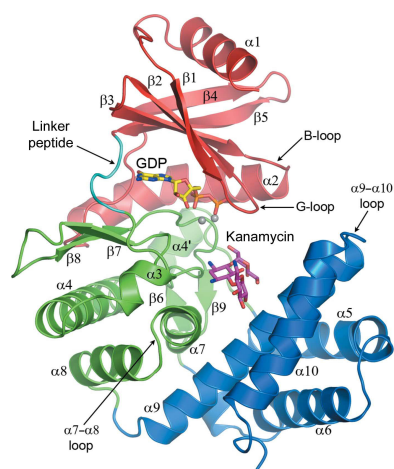
Keywords: crystal structure; aminoglycosides; phosphotransferases; antibiotic resistance.

PDB reference: GDP and kanamycin complex of APH(2'')-IIIa, 6ctz

Aminoglycoside phosphotransferases (APHs) are one of three families of aminoglycoside-modifying enzymes that confer high-level resistance to the aminoglycoside antibiotics via enzymatic modification. This has now rendered many clinically important drugs almost obsolete. The APHs specifically phosphorylate hydroxyl groups on the aminoglycosides using a nucleotide triphosphate as the phosphate donor. The APH(2'') family comprises four distinct members, isolated primarily from *Enterococcus* sp., which vary in their substrate specificities and also in their preference for the phosphate donor (ATP or GTP). The structure of the ternary complex of APH(2'')-IIIa with GDP and kanamycin was solved at 1.34 Å resolution and was compared with substrate-bound structures of APH(2'')-Ia, APH(2'')-IIa and APH(2'')-IVa. In contrast to the case for APH(2'')-Ia, where it was proposed that the enzyme-mediated hydrolysis of GTP is regulated by conformational changes in its N-terminal domain upon GTP binding, APH(2'')-IIa, APH(2'')-IIIa and APH(2'')-IVa show no such regulatory mechanism, primarily owing to structural differences in the N-terminal domains of these enzymes.

1. Introduction

The aminoglycosides comprise a family of broad-spectrum bactericidal antibiotics that are used for the treatment of serious bacterial infections in humans (Gilbert, 2010), and are also utilized for growth promotion and treatment of animals in veterinary practice (Cantas *et al.*, 2013). Their cellular target is the A-site of the 30S ribosomal subunit (Vicens & Westhof, 2003; Fourmy *et al.*, 1996), where aminoglycoside binding impairs proofreading during translation and results in the disruption of protein synthesis (Carter *et al.*, 2000). The aminoglycoside family includes a wide array of structurally diverse compounds that share a central aminocyclitol ring (the B ring) decorated with one, two or three glycan side groups (the A, C and D rings; Becker & Cooper, 2013; Majumder *et al.*, 2007). They are divided into three major groups: 4,5-disubstituted, 4,6-disubstituted and atypical compounds (Supplementary Fig. S1). The 4,5-disubstituted aminoglycosides are represented by neomycin, paromomycin, lividomycin and butirosin. The 4,6-disubstituted aminoglycosides include most of the clinically important drugs such as kanamycin, amikacin, gentamicin, isepamicin, tobramycin and arbekacin, while atypical aminoglycosides are exemplified by streptomycin, spectinomycin and apramycin. The A and B rings in



the 4,5-disubstituted and 4,6-disubstituted aminoglycosides generally have a moderately conserved structure, and this two-ring group is known as the neamine or neamine-like moiety (Supplementary Fig. S1). It is this neamine group which is responsible for the recognition of the target RNA A-site (Vicens & Westhof, 2003; Fourmy *et al.*, 1996).

There is currently such widespread resistance to these antibiotics in most bacteria, owing to diminished cell entry, active efflux, target alteration and enzymatic inactivation or modification of the drugs (Davies & Davies, 2010; De Pascale & Wright, 2010; Ramirez & Tolmasky, 2010; Smith & Baker, 2002; Wright, 1999, 2003; Wright *et al.*, 1998), that many of them have reduced relevance in a clinical setting. Enzymatic modification of aminoglycosides leading to reduced affinity for the 30S ribosomal target is the major mechanism of resistance to these drugs. This modification results from the activity of three distinct families of bacterially encoded aminoglycoside-modifying enzymes: the acetyl-coenzyme A-dependent aminoglycoside acetyltransferases (AACs), the ATP-dependent nucleotidyltransferases (ANTs) and the ATP/GTP-dependent phosphotransferases (APHs).

The APH enzymes confer resistance to aminoglycosides by transferring the γ -phosphate moiety of ATP or GTP to a free hydroxyl group on the aminocyclitol ring or the glycan rings. They are grouped into subfamilies depending upon which hydroxyl is modified. The APH(2'') family, for example, includes seven enzymes, APH(2'')-Ia, APH(2'')-IIa, APH(2'')-IIIa and APH(2'')-IVa (Toth *et al.*, 2009), APH(2'')-Ie (Mahbub Alam *et al.*, 2005), APH(2'')-If (Toth *et al.*, 2013) and APH(2'')-Ig (Chen *et al.*, 2013), which phosphorylate the free hydroxyl group at the 2'' position on the C ring of aminoglycosides such as gentamicin and kanamycin (Supplementary Fig. S1). APH enzymes are structurally related to the catalytic domains of the eukaryotic protein kinases (Hon *et al.*, 1997), particularly with respect to the nucleotide-binding site and the anchoring of the triphosphate moiety. However, unlike protein kinases, the phosphoryl-transfer reaction of which is tightly regulated (Johnson *et al.*, 1996, 1998; Endicott *et al.*, 2012), the APH enzymes are deemed to be essentially unregulated since they lack most of the kinase regulatory machinery (Davies & Wright, 1997; Caldwell *et al.*, 2016). For some APH enzymes it has been demonstrated that apart from their major function, the phosphorylation of aminoglycosides, they continuously hydrolyze bound NTPs in the absence of the antibiotic substrate. This phenomenon was first demonstrated for the APH(3'')-Ia and APH(3'')-IIa enzymes. They perform continuous basal-level ATP hydrolysis irrespective of whether an aminoglycoside substrate is present or not, which imposes a significant cost to the bacteria harboring the *aph(3'')* gene (Kim *et al.*, 2006). Subsequently, it was shown that two members of the APH(2'') family, APH(2'')-Ia (Fraser *et al.*, 2012) and APH(2'')-IIIa (Badarau *et al.*, 2008), also have a continuous intrinsic level of GTP hydrolysis in the absence of a substrate.

Recent structural studies with APH(2'')-Ia suggest that in this particular enzyme nucleotide hydrolysis may be regulated by conformational changes (Caldwell *et al.*, 2016). In the

absence of aminoglycoside antibiotics, the triphosphate moiety of the bound GTP is held in a stabilized, inactive state and it is likely that in this state adventitious hydrolysis and transfer of the γ -phosphate to water may be minimized. The binding of antibiotic results in a conformational change in the enzyme, which triggers the conversion of the triphosphate into an active, catalytically competent conformation capable of initiating the phosphorylation of aminoglycoside substrates. It is not known whether the other APH(2'') enzymes share this regulatory mechanism that restricts wasteful NTP hydrolysis in the absence of a substrate. To address this issue, we have determined the X-ray crystal structure of the ternary complex of APH(2'')-IIIa with Mg₂GDP and kanamycin, and have performed detailed comparative analyses of the four available APH(2'') structures. This study revealed significant differences in the structural elements responsible for the enzyme-mediated NTP hydrolysis by individual APH(2'') enzymes and demonstrated that the regulatory mechanism described for APH(2'')-Ia does not exist in APH(2'')-IIa, APH(2'')-IIIa and APH(2'')-IVa phosphotransferases.

2. Materials and methods

2.1. Protein purification and crystallization

The APH(2'')-IIIa protein was expressed and purified as described in Byrnes *et al.* (2008). Briefly, the wild-type *aph(2'')-IIIa* gene and its mutant derivative that results in an F108L substitution were cloned into the pET-22a vector (Novagen) and expressed in *Escherichia coli* BL21(DE3) cells. The proteins were purified on kanamycin and gentamicin affinity columns eluted using a linear gradient of 0–1 M NaCl in 25 mM HEPES pH 7.5, 0.2 mM DTT, 1 mM EDTA as described previously (Kim *et al.*, 2004). As described in previous structural studies of APH(2'')-IIIa (Smith *et al.*, 2012), the F108L point mutant was used since it crystallized more readily than the wild-type enzyme and gave large diffraction-quality crystals. The ternary complex was prepared by adding a tenfold molar excess of Mg₂GTP and kanamycin to the apo APH(2'')-IIIa F108L enzyme, followed by incubation of the complex at 4°C for 2 h. The complex was crystallized from 30% PEG 4000, 0.1 M Tris–HCl pH 8.5.

2.2. Diffraction data collection and structure solution

Data were collected on beamline 7-1 at Stanford Synchrotron Radiation Lightsource (SSRL) using X-rays at 12 658 eV (0.97946 Å). A total of 1440 images were collected with an oscillation range of 0.25° and an exposure time of 2.5 s. The data were processed with *XDS* (Kabsch, 2010) and scaled with *AIMLESS* (Evans & Murshudov, 2013) to give a final unique data set comprising 73 245 reflections to 1.34 Å resolution. Additional data-collection statistics are given in Table 1.

The structure of the APH(2'')-IIIa ternary complex was solved by molecular replacement with *MOLREP* (Vagin & Teplyakov, 2010) from the *CCP4* suite (Winn *et al.*, 2011) using the binary Mg₂GDP–APH(2'')-IIIa complex as the starting model (PDB entry 3tdw; Smith *et al.*, 2012) with the cofactor

Table 1

Data-collection statistics.

Values in parentheses are for the outer shell.

Space group	$P2_12_12$
Unit-cell parameters (Å)	$a = 77.169, b = 58.982, c = 70.853$
Resolution range (Å)	39.08–1.34 (1.38–1.34)
Observed reflections	1059048 (48437)
Unique reflections to 1.34 Å resolution	73245 (3558)
R_{meas} (%)	6.3 (108.2)
$R_{\text{p.i.m.}}$ (%)	1.7 (29.0)
$\langle I/\sigma(I) \rangle$	22.1 (2.7)
Completeness (%)	100 (99.6)
$CC_{1/2}$	0.999 (0.81)
Multiplicity	14.3 (13.9)
Wilson B factor (Å ²)	14.7

Table 2

Structure-refinement statistics.

R factor/ $R_{\text{free}}^{\dagger}$ (%)	14.58/17.09
Total No. of atoms	
Protein	2468
Solvent	380
R.m.s.d. from ideality	
Bond distances (Å)	0.005
Bond angles (°)	0.91
Atomic displacement parameters (Å ²)	
Protein	20.6
Solvent	33.6
GDP	13.3
Kanamycin	18.8
Fit of ligands to density	
Occupancy (%)	100 (GDP), 100 (kanamycin)
RSCC \ddagger	0.98 (GDP), 0.96 (kanamycin)
Ramachandran plot \S	
Residues in favored regions (%)	98.3
Outliers	0
$MolProbity$ score	1.25 (94th percentile)
PDB code	6ctz

\dagger R_{free} was calculated with a randomly chosen 5% of the reflections. \ddagger From the PDB validation report. \S Calculated with *MolProbity* (Chen *et al.*, 2010).

and water molecules removed. The structure was initially refined with *REFMAC* (Murshudov *et al.*, 2011), and the Mg_2GDP and kanamycin were added into residual $F_o - F_c$ electron density with *Coot* (Emsley *et al.*, 2010). Water molecules were added in chemically relevant positions. Structure refinement was completed with *phenix.refine* (Adams *et al.*, 2010), in which all atoms were refined with anisotropic atomic displacement parameters (ADPs). The final structure comprised residues 5–301, with the first four residues and the last five residues omitted owing to a lack of electron density. The final crystallographic R factor and R_{free} were 0.1458 and 0.1709, respectively. All structure-refinement statistics are given in Table 2.

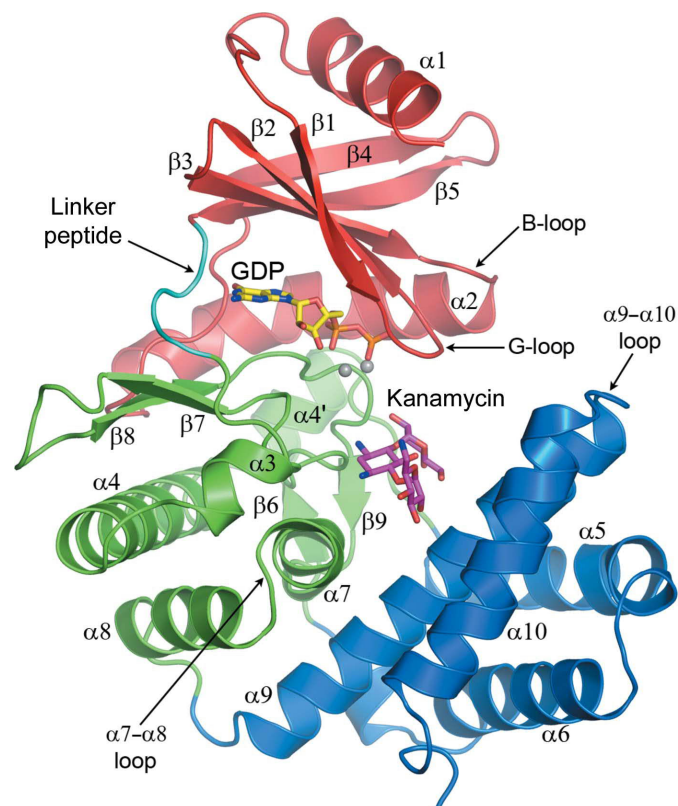
3. Results and discussion

3.1. The structure of the APH(2'')-IIIa ternary complex

The structure of the F108L mutant of APH(2'')-IIIa has been reported previously as the binary Mg_2GDP complex (Smith *et al.*, 2012). Briefly, the F108L APH(2'')-IIIa enzyme [hereafter referred to simply as APH(2'')-IIIa since the point-mutant and wild-type enzymes have the same structure; Smith

et al. (2012)] is composed of two domains: an N-terminal domain (residues 5–93) comprising a central five-stranded β -sheet ($\beta 1$ – $\beta 5$) flanked by two helices ($\alpha 1$ and $\alpha 2$) and a C-terminal domain (99–301), with a five-residue linker peptide (94–98) connecting the two domains. The C-terminal domain can be further divided into two non-contiguous subdomains: the core subdomain (residues 99–142 and 189–252) comprising four α -helices ($\alpha 3$, $\alpha 4$, $\alpha 7$ and $\alpha 8$) and a long β -finger motif ($\beta 7$ and $\beta 8$), and the helical subdomain (residues 143–188 and 253–301) made up of four antiparallel α -helices ($\alpha 5$, $\alpha 6$, $\alpha 9$ and $\alpha 10$) (Fig. 1).

The ternary complex between APH(2'')-IIIa, GDP and kanamycin can be regarded as an inactive abortive complex, since the γ -phosphate group which would normally be transferred to the 2''-hydroxyl of the substrate is absent. The cofactor binding in the ternary complex is similar in detail to that in the previously described binary complex (Smith *et al.*, 2012). Briefly, the guanine moiety forms two hydrogen bonds to the specificity template formed by the linker peptide between the N- and C-terminal domains, with a third hydrogen bond to the $\text{O}^{\prime\prime}$ atom of the gatekeeper residue Tyr92 (Supplementary Fig. S2a). The diphosphate group is anchored by hydrogen bonds to residues from the G-loop (a flexible loop between strands $\beta 1$ and $\beta 2$) from the N-terminal domain, reminiscent of other aminoglycoside phosphotransferases and

**Figure 1**

A ribbon representation of APH(2'')-IIIa showing the three structural domains: the N-terminal domain (red), the central core subdomain (green) and the helical subdomain (blue). The locations of the GDP (yellow sticks) and kanamycin (magenta sticks) are shown, along with the linker peptide (cyan) responsible for selectivity of the nucleotide and several loops important in substrate binding and regulation.

protein kinases, and to highly conserved residues from the core subdomain (not shown). Two magnesium ions are also present in the binding site, one bridging between O atoms of the α - and β -phosphates and the second coordinated to the β -phosphate only. Final electron density for the Mg_2GDP complex is given in Supplementary Fig. S2(a).

The aminoglycoside-binding site is located within a deep cleft between the core and helical subdomains (Fig. 1). The kanamycin molecule was built into strong residual $F_o - F_c$ density (Fig. 2a) and the final $2F_o - F_c$ electron density is shown in Supplementary Fig. S2(b). The substrate-binding site can be divided into three distinct regions representing the catalytic loop (motif 1; Asp196, Ser198 and Asp221), the loop between helices $\alpha 7$ and $\alpha 8$ (motif 2; Glu236 and Asp237) and the $\alpha 9$ helix (motif 3; Asp269, Gln270 and Tyr273) (Fig. 2b). The kanamycin substrate makes a total of 12 hydrogen-bonding interactions with the protein, two-thirds of them with the core subdomain (Fig. 2b and Supplementary Table S1). The aminoglycoside is orientated such that the C ring carrying the 2''-hydroxyl group is within hydrogen-bonding distance (2.74 Å) of the $\text{O}^{\delta 2}$ atom of Asp196, the putative catalytic base. The central B ring projects towards the core subdomain and makes four hydrogen bonds to residues from motif 1 (Asp196 and Ser198) and motif 2 (Asp237). At the base of the binding cleft, the A ring is directed across the cleft towards the helical subdomain and makes three hydrogen-bonding inter-

actions with two residues of motif 3 (Asp269 and Gln270) on helix $\alpha 9$ and two interactions with Glu236 of motif 2 on the core subdomain. A total of 13 ordered water molecules make additional interactions with the kanamycin (Supplementary Table S1 and Fig. 2b), either bridging to the protein or making contact only with the substrate. The highly polar nature of the aminoglycosides (kanamycin, for example, has seven hydroxyl groups and four amino groups, the latter of which are all protonated under physiological conditions; Setny & Trylska, 2009) dictates that these molecules have a high propensity for hydrogen bonding, and that prior to binding they would be surrounded by a hydration shell which would be somewhat retained upon APH binding. This is observed in most APH-aminoglycoside complexes, where between five and 15 water molecules are hydrogen-bonded to the bound substrates.

Superposition of the ternary complex onto the binary $\text{Mg}_2\text{GDP-APH}(2'')\text{-IIIa}$ complex (PDB entry 3tdw) gives an r.m.s.d. of 0.9 Å for 296 matching C^α atoms, and while this implies that there are no major conformational differences between the two structures, when the N-terminal domain and the core and helical subdomains were superimposed separately, the r.m.s.d.s were slightly lower at 0.7, 0.5 and 0.7 Å, respectively. This suggests that there could be a difference in the relative orientations of the domains, and such a difference can be seen when the structures are superimposed based upon the core subdomain only (Supplementary Fig. S3). It appears

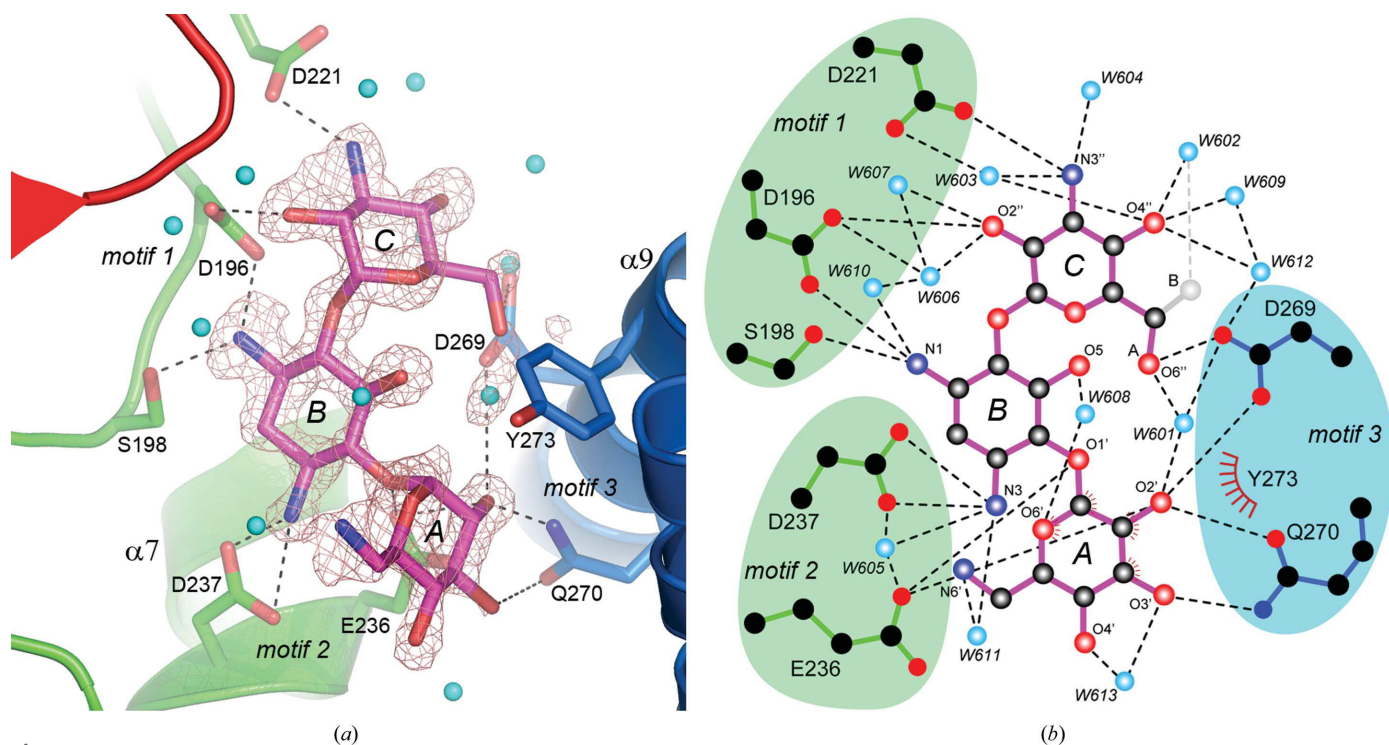


Figure 2
 (a) Initial $F_o - F_c$ density (pink mesh at 2.5σ) for kanamycin in the APH(2'')-IIIa ternary complex. The final refined position for the kanamycin is shown as magenta sticks. The N-terminal domain and the core and helical subdomains are colored using the same color scheme as in Fig. 1 (red, green and blue, respectively). Hydrogen-bonding interactions between the kanamycin and the protein are shown as dashed lines. Water molecules within hydrogen-bonding distance of the kanamycin are indicated by small cyan spheres, but the hydrogen bonds are omitted for clarity. (b) The full hydrogen-bonding network surrounding kanamycin (magenta). Residues from the core subdomain are colored green and those from the helical subdomain are colored blue. The three sequence motifs associated with substrate binding are indicated as colored patches. Water molecules are indicated as cyan circles. The $\text{O}6''$ atom on the C ring of kanamycin was built into two alternate conformations (A and B). The A conformer has a refined occupancy of 0.65 and is colored red, while the B conformer with an occupancy of 0.35 is colored gray.

that both the N-terminal domain and the helical subdomain may have rotated slightly closer to the core subdomain in the ternary APH(2'')-IIIa complex by an estimated 1–2° for both. These domain movements are too small to be deemed significant and could possibly be attributed to differences stemming from the crystallization conditions and crystal packing. Hence, we conclude that kanamycin binding does not induce any appreciable opening or closing of the substrate-binding cleft in APH(2'')-IIIa.

3.2. Comparison with the other APH(2'') enzymes

While the overall structures of the four APH(2'') aminoglycoside phosphotransferases are topologically similar, the

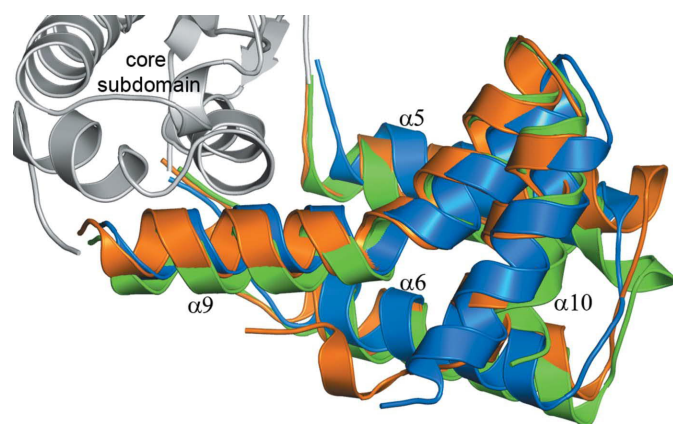


Figure 3
Comparison of the helical subdomains of APH(2'')-Ia (blue; PDB entry 4ork), APH(2'')-IIa (orange; PDB entry 3ham) and APH(2'')-IVa (green; PDB entry 3sg9). The three structures were all superimposed onto APH(2'')-IIIa based on the core subdomain, which is shown only for APH(2'')-IIIa (gray).

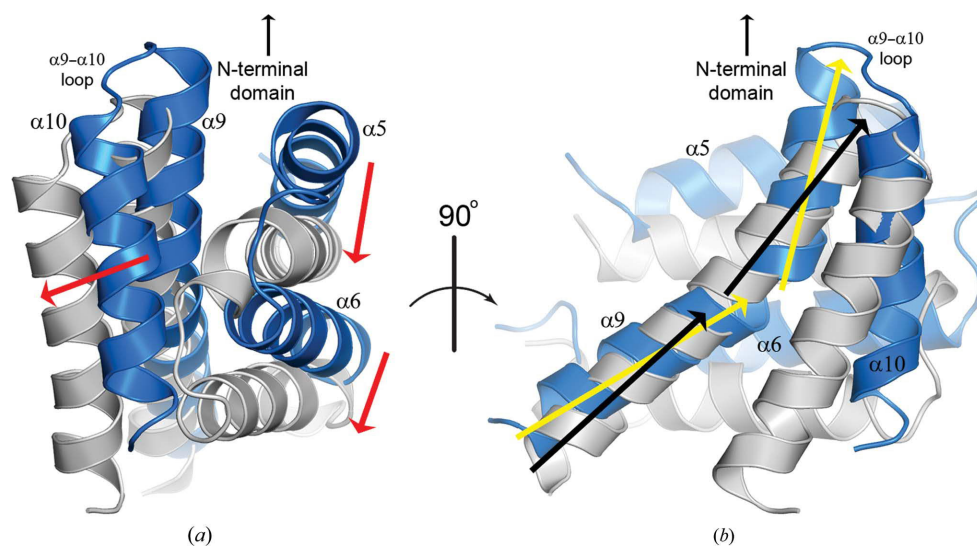


Figure 4
Comparison of the helical subdomains of APH(2'')-IIIa (gray) and APH(2'')-Ia (blue; PDB entry 4ork) resulting from a superposition of the two structures based on the core subdomain (not shown). In (a), the red arrows indicate the approximate relative direction of movement of the $\alpha 5$, $\alpha 6$ and $\alpha 10$ helices. In (b), the view has been rotated 90° about a vertical axis. The difference in the structure of the $\alpha 9$ helix is indicated by two black arrows which indicate a slight nonlinearity of the helix in APH(2'')-IIIa and by two yellow arrows which indicate the substantial bend in the helix in APH(2'')-Ia.

superposition of the ternary APH(2'')-IIIa complex onto the structures of APH(2'')-Ia (PDB entry 4ork; Smith *et al.*, 2014), APH(2'')-IIa (PDB entry 3ham; Young *et al.*, 2009) and APH(2'')-IVa (PDB entry 3sg9; Shi *et al.*, 2011) shows that the relative spatial arrangement of their subdomains varies substantially. The overall r.m.s.d.s for APH(2'')-Ia, APH(2'')-IIa and APH(2'')-IVa, relative to APH(2'')-IIIa, are 2.8, 2.3 and 2.4 Å, respectively, whereas the individual domain r.m.s.d.s are generally lower, with the notable exception of the helical subdomains (Supplementary Table S2). Compared with both APH(2'')-IIa and APH(2'')-IVa, the helical subdomain of APH(2'')-IIIa has a higher r.m.s.d. than the overall average, indicating a significant difference between the enzymes in this part of the structure. The APH(2'')-Ia, APH(2'')-IIa and APH(2'')-IVa enzymes show a somewhat better overall structural agreement between themselves than with APH(2'')-IIIa, with r.m.s.d.s ranging from 1.6 to 2.1 Å (Supplementary Table S2). The variation in structure is essentially mirrored in the sequence identities between the four enzymes. The four enzymes for which structures are known all have rather low levels of sequence identity to each other (24–32%).

When APH(2'')-IIIa is superimposed on the other three APH(2'') enzymes based upon the core subdomain only, the differences in the relative positions of the N-terminal domains and the helical subdomains can be better appreciated (Supplementary Fig. S4). It is apparent that, at least with regard to the structure and location of the helical subdomain, APH(2'')-IIIa is the most divergent of the four enzymes. Individually, the helical subdomains of APH(2'')-Ia, APH(2'')-IIa and APH(2'')-IVa superimpose very well onto each other via a small rigid-body rotation and translation of the entire domain (Fig. 3). However, the relative difference of the helical subdomains between APH(2'')-IIIa and the other APH(2'')

enzymes does not appear to be a simple rigid-body rotation/translation but rather a screw-like displacement approximately about the axis of the $\alpha 9$ helix (Fig. 4a). The $\alpha 5$ – $\alpha 6$ and $\alpha 9$ – $\alpha 10$ pairs of helices are offset in different directions and by varying distances, such that a single rigid-body superposition of the APH(2'')-IIIa helical domain onto the other three enzymes gives a rather poor overlap of the helices and hence larger r.m.s.d.s. This difference in the orientation of the helical domain of APH(2'')-IIIa relative to the other APH(2'') enzymes can be viewed as a lateral sliding of the $\alpha 5$ – $\alpha 6$ pair en bloc by about 7 Å in a direction almost parallel to the axis of the $\alpha 9$ helix (Fig. 4a). Upon superposition, the $\alpha 9$ – $\alpha 10$ pairs of these two enzymes are

separated by approximately 4–5 Å along the axis of the $\alpha 9$ helix (Fig. 4). The long $\alpha 9$ helix is almost straight in APH(2'')-IIIa, whereas it is markedly kinked at approximately the halfway point in an almost identical manner in the other APH(2'') enzymes (Fig. 4b). The relative translation of the domain, coupled with this straightening of the $\alpha 9$ helix in APH(2'')-IIIa, serves to reposition the C-terminal end of this helix and the $\alpha 9$ - $\alpha 10$ loop which follows significantly further from the N-terminal domain relative to the other three APH(2'') enzymes.

3.3. Substrate binding in the APH(2'') enzymes

Comparison of all four APH(2'') enzymes shows that the substrate molecules are bound in essentially the same orientation in all structures. The neamine moiety of aminoglycosides is nestled against the core subdomain and helix $\alpha 9$ such that the A ring projects towards motif 3 in the helical subdomain and the B ring points towards motif 1 and motif 2 in the core subdomain. The C ring then projects back towards the helical domain (Figs. 2a and 5a).

Motif 1 is structurally and sequentially conserved in the four APH(2'') enzymes, with motif 2 and motif 3 showing some variability (Fig. 5b). In APH(2'')-IIIa, motif 2 comprises two residues (Glu236 and Asp237) from helix $\alpha 7$ (Figs. 5a and 5c) just prior to the short $\alpha 7$ - $\alpha 8$ turn. There is a marked difference in this motif in the other three enzymes. In APH(2'')-Ia and APH(2'')-IIa the last two residues of helix $\alpha 7$ have unwound and four additional residues are inserted, resulting in an extended $\alpha 7$ - $\alpha 8$ loop. In APH(2'')-IVa this insertion comprises three additional residues (Figs. 5b and 5c). Motif 2 in all four enzymes contributes either two or three residues to substrate binding. In the helical domain, a conserved aromatic residue in motif 3 [tyrosine in APH(2'')-Ia and APH(2'')-IIIa (Tyr273 in Fig. 2), tryptophan in APH(2'')-IIa and APH(2'')-IVa] makes a face-to-face hydrophobic interaction with the A ring. In all four enzymes, the side chain of the amino acid preceding this aromatic residue by one turn of helix is in a position to make a hydrogen-bonding interaction with the A ring of the bound substrate [glutamate in APH(2'')-Ia and APH(2'')-IVa, aspartate in APH(2'')-IIa and glutamine in APH(2'')-IIIa; Fig. 2]. Owing to the difference in the structure and position of the $\alpha 9$ helix in APH(2'')-IIIa, this enzyme has a third residue in motif 3 (Asp269) which forms additional hydrogen bonds to the A ring and C ring (Fig. 2).

In APH(2'')-IIIa the straightening of the $\alpha 9$ helix and the movements of the $\alpha 5$, $\alpha 6$ and $\alpha 10$ helices described above result in a movement of the motif 3 residues by about 4 Å on average in a direction along the length of the $\alpha 9$ helix and towards the core subdomain. This in turn places the side chain of Gln270 on motif 3 further into the aminoglycoside pocket, forcing the A ring to move closer to the core subdomain and constraining the A ring significantly more than in the other three enzymes. The structural differences observed in this region of the substrate-binding pocket in APH(2'')-IIIa could result in a tighter anchoring of the A ring compared with the other three APH(2'') enzymes, which may ultimately be

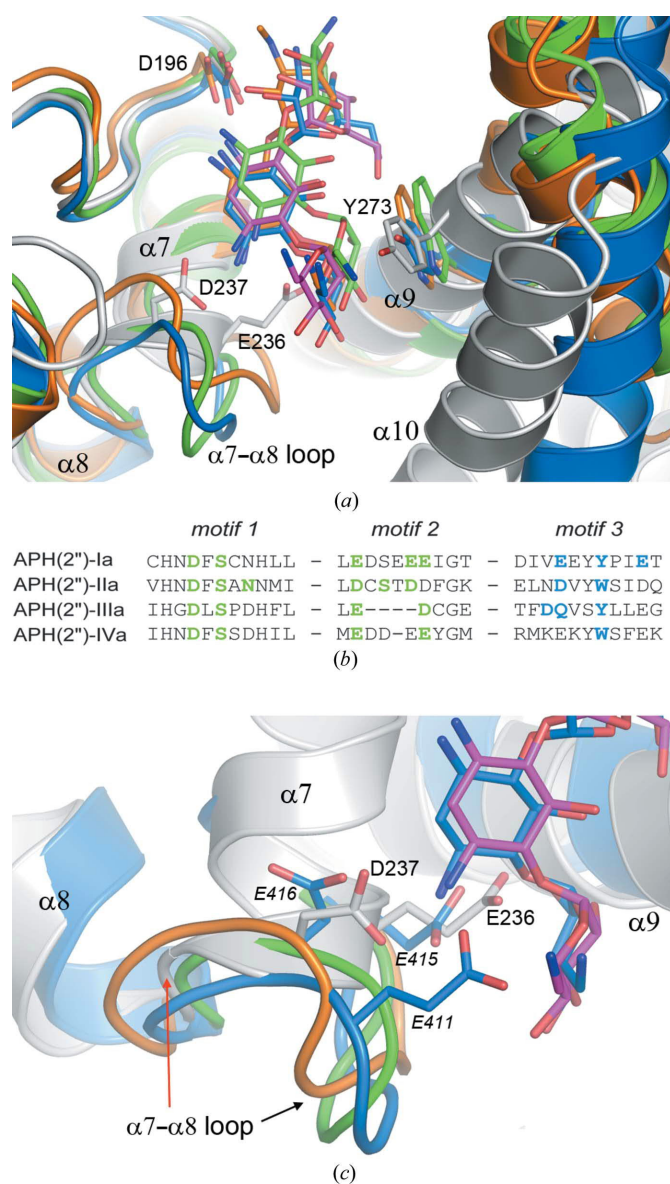


Figure 5

(a) The location of the kanamycin substrates in APH(2'')-Ia (blue sticks; PDB entry 5iqb), APH(2'')-IIIa (magenta sticks) and APH(2'')-IVa (green sticks; PDB entry 3sg9) and of gentamicin in APH(2'')-IIa (orange sticks; PDB entry 3ham). The four structures were superimposed based on residues in the core subdomain, which is on the left of the panel. The corresponding helical subdomains are on the right side of the panel, colored blue [APH(2'')-Ia], orange [APH(2'')-IIa], gray [APH(2'')-IIIa] and green [APH(2'')-IVa]. (b) Partial sequence alignment of APH(2'')-Ia, APH(2'')-IIa, APH(2'')-IIIa and APH(2'')-IVa. The three sequence motifs associated with aminoglycoside substrate binding are shown. Residues which form hydrogen-bonding interactions with the substrates for each enzyme are colored green for those from the core subdomain and blue for those from the helical subdomain. (c) The $\alpha 7$ - $\alpha 8$ loop (motif 2) in APH(2'')-Ia (blue; PDB entry 5iqb), APH(2'')-IIa (orange; PDB entry 3ham), APH(2'')-IIIa (gray) and APH(2'')-IVa (green; PDB entry 3sg9). This loop in APH(2'')-IIIa is a short two-residue turn indicated by the red arrow, whereas it is 3–4 residues longer in the three other APH(2'') enzymes (black arrow). The motif 2 residues in APH(2'')-Ia (blue sticks) and APH(2'')-IIIa (gray sticks) are shown, and those from APH(2'')-IIa and APH(2'')-IVa are omitted for clarity. The kanamycin substrates for APH(2'')-Ia (blue) and APH(2'')-IIIa (magenta) are also shown.

important in the selection of the aminoglycoside substrates that can bind in this site.

3.4. Mechanism of the phosphorylation of aminoglycoside antibiotics by APH(2'') enzymes

In a recent structural study of APH(2'')-Ia, it was demonstrated that in the absence of bound substrate the enzyme adopts a conformation that minimizes spontaneous GTP hydrolysis (Caldwell *et al.*, 2016). In complexes of APH(2'')-Ia with the nonhydrolyzable nucleotide analog GMPPNP (PDB entries 5iqb, 5iqc, 5iqd and 5iqe; Caldwell *et al.*, 2016), residues from the G-loop and the B-loop (which is adjacent to the G-loop and connects strand $\beta 3$ and helix $\alpha 2$) in the N-terminal domain interact with the triphosphate moiety of the nucleotide and maintain it in an elongated (non-active) configuration. The G-loop was deemed to be in an open conformation when the enzyme was in this state. In this configuration of the triphosphate, the terminal γ -phosphate group is over 6.5 Å from the 2''-hydroxyl of a bound aminoglycoside and oriented such that phosphorylation would not be favored. Aminoglycoside binding to APH(2'')-Ia results in the rearrangement of the triphosphate-binding site, which is communicated via interactions between helix $\alpha 9$ from the helical subdomain and the B-loop and G-loops on the N-terminal domain, resulting in the closure of the G-loop over the triphosphate moiety. Consequently, the triphosphate adopts a new configuration such that the γ -phosphate group projects towards the 2''-hydroxyl receptor on the substrate and is about 4 Å away. It was proposed that the non-active conformation of the triphosphate of NTP prevents its spontaneous hydrolysis in the absence of the aminoglycoside substrate, and the binding of a substrate results in the transition of the triphosphate into the active conformation required for phosphoryl transfer to aminoglycoside antibiotics (Caldwell *et al.*, 2016; Ngo & Garneau-Tsodikova, 2016).

To appreciate whether the spontaneous hydrolysis of GTP by APH(2'')-IIIa is similarly regulated, we undertook a detailed comparison of APH(2'')-Ia and APH(2'')-IIIa. Examination of the structures shows that the non-active

conformation described for APH(2'')-Ia is not observed in APH(2'')-IIIa. Unlike in APH(2'')-Ia, the G-loop is in the closed conformation in APH(2'')-IIIa, and this is a direct consequence of the alternative folding of its B-loop (Fig. 6). In APH(2'')-Ia the B-loop comprises seven residues between strand $\beta 3$ and helix $\alpha 2$ and is essentially unstructured and meandering, extending out from the N-terminal domain towards the helical domain. In APH(2'')-IIIa, helix $\alpha 2$ is one and a half turns longer than in APH(2'')-Ia, and consequently the B-loop comprises only two residues involved in a very tight turn between strand $\beta 3$ and helix $\alpha 2$ (Fig. 6). The extra turn of helix $\alpha 2$ in APH(2'')-IIIa forces the G-loop into the closed conformation and would prevent any transition into an open conformation. A single aromatic interaction between the side chains of Phe31 from the G-loop and Trp285 from helix $\alpha 10$, which is present irrespective of the occupancy of the aminoglycoside-binding site (Supplementary Figs. S5a and S5b), serves to lock the G-loop into this closed conformation over the bound nucleotide. In APH(2'')-IIIa, the shorter B-loop precludes any interaction with the helical domain and the triphosphate moiety of GTP, and severs all communication between the substrate- and nucleotide-binding sites. Moreover, there are no direct hydrogen-bonding interactions between the helical subdomain and the N-terminal domain (either in the presence or absence of the substrate) owing to the straightening of the $\alpha 9$ helix and the rigid-body twisting of the helical subdomain described above in Section 3.2. This is in contrast to APH(2'')-Ia, in which both the B-loop and G-loop are involved in extensive interactions with the helical subdomain (Supplementary Fig. S5c). Combined, these data indicate that unlike in APH(2'')-Ia, there is no inactive GTP conformation in APH(2'')-IIIa to minimize spontaneous hydrolysis. Furthermore, a GTP-activation mechanism involving direct communication between the substrate- and nucleotide-binding sites via the B-loop, as described for APH(2'')-Ia, would not be applicable in APH(2'')-IIIa.

With regard to APH(2'')-IIa and APH(2'')-IV, structures of the former are available as apo and ADP-bound forms (PDB entries 3uzr and 4dca; Center for Structural Genomics of Infectious Diseases, unpublished work), the binary gentamicin complex (PDB entry 3ham; Young *et al.*, 2009) and the ternary complex with ATP and streptomycin (PDB entry 3hav; Young *et al.*, 2009), an atypical aminoglycoside that is not a substrate of the enzyme (Young *et al.*, 2009), while only apo and binary nucleotide or aminoglycoside complexes of APH(2'')-IVa have been described (Shi & Berghuis, 2012; Shi *et al.*, 2011; Toth *et al.*, 2010). Structural comparison of these two enzymes with APH(2'')-Ia and APH(2'')-IIIa shows that the B-loops in APH(2'')-IIa and APH(2'')-IVa are short and isostructural with APH(2'')-IIIa (Supplementary Fig. S6), such that a regulatory mechanism involving this loop, similar to that described for APH(2'')-Ia, would also be precluded in

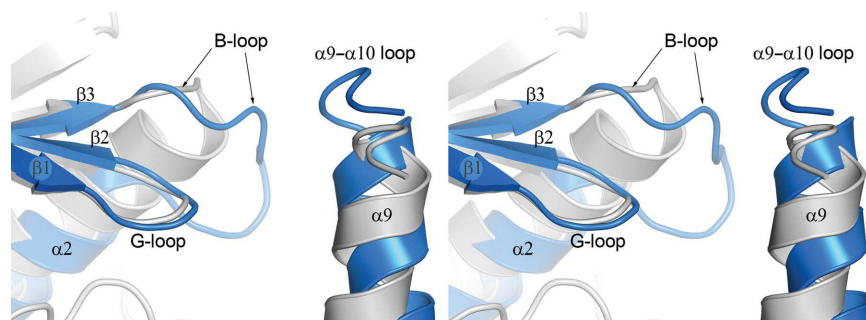


Figure 6

Stereoview of the interface between the N-terminal domain (left) and the helical subdomain (right) for APH(2'')-IIIa (gray) and APH(2'')-Ia (PDB entry 4ork; blue). The extended B-loop in APH(2'')-Ia is indicated, as is the significantly shorter B-loop in APH(2'')-IIIa resulting from the additional one and a half turns of helix $\alpha 2$. The difference in the position of the $\alpha 9$ - $\alpha 10$ loop following straightening and translation of the $\alpha 9$ helix in APH(2'')-IIIa can be seen.

these two enzymes. Hence, the available structural data suggest that APH(2'')-Ia is the only one of the four APH(2'') enzymes whose intrinsic hydrolysis of NTP can potentially be regulated, and in which the aminoglycoside phosphorylation event is triggered by communication between the substrate- and nucleotide-binding sites.

3.5. Intrinsic nucleotide hydrolysis in the APH(2'') enzymes

Previous kinetic studies have demonstrated that both APH(2'')-Ia (Frase *et al.*, 2012) and APH(2'')-IIIa (Badarau *et al.*, 2008) have equal intrinsic GTPase activities ($k_{\text{cat}} = 0.012 \text{ s}^{-1}$), and APH(2'')-IVa also has a basal ATPase activity with a k_{cat} of 0.014 s^{-1} (Kaplan *et al.*, 2016). In all cases it is assumed that the γ -phosphate of the nucleotide is transferred to water. Similar residual levels of ATPase activity ($k_{\text{cat}} = 0.02 \text{ s}^{-1}$) have previously been observed for members of the APH(3') subfamily, and it was demonstrated that wasteful GTP hydrolysis by these enzymes is evolutionarily disadvantageous for bacteria (Kim *et al.*, 2006). The observation that the GTP complexes of APH(2'')-Ia (Caldwell *et al.*, 2016; Smith *et al.*, 2014) and APH(2'')-IIIa (Smith *et al.*, 2012) have electron density consistent with GDP confirms that hydrolysis has occurred in the absence of substrate. This implies that spontaneous hydrolysis in APH(2'')-Ia occurs irrespective of whether the triphosphate is in the active or the stabilized configuration, and that the observed stabilization may serve only to provide regulation or enhancement of the actual phosphorylation event itself, once the substrate has bound. It is also possible that APH(2'')-Ia could have a higher intrinsic level of spontaneous GTP hydrolysis than the other APH(2'') enzymes, and that the regulatory mechanism described by Caldwell *et al.* (2016) is necessary to bring the level down to the level observed for other APH phosphotransferases to circumvent excessive wasteful hydrolysis.

It has also been shown that some aminoglycosides, which are not substrates (neamine, apramycin, neomycin B and paromomycin) but could act as inhibitors of APH(2'')-Ia and APH(2'')-IIIa, are capable of further elevating the basal GTPase activity of these enzymes (Badarau *et al.*, 2008; Frase *et al.*, 2012). In APH(2'')-Ia, this elevation (between 2.5-fold and sevenfold) of the intrinsic GTPase activity upon neamine, neomycin B and paromomycin binding (Frase *et al.*, 2012) may result from a conformationally induced switch of the GTP from the stabilized to the activated configuration in a manner similar to that described above, resulting in a higher rate of γ -phosphate transfer to a water molecule. The increase in intrinsic GTPase activity in APH(2'')-IIIa by approximately threefold in the presence of the nonsubstrates neamine and apramycin (Badarau *et al.*, 2008) is indicative of a different mechanism, since our ternary structure of this enzyme shows that the conformation of the nucleotide-binding site is uncoupled from any conformational changes occurring in the helical subdomains induced by inhibitor binding.

4. Conclusion

Structural analyses of the APH(2'') enzymes show that despite similarities in their three-dimensional structures and the

conservation of key sequence motifs, they display a spectrum of structural responses to nucleotide and aminoglycoside binding. Enzyme-mediated spontaneous GTP hydrolysis in APH(2'')-Ia has been proposed to be regulated to a certain extent by specific conformational changes in the N-terminal domain, with targeted aminoglycoside phosphorylation triggered by inter-domain communication upon substrate binding, mediated by an extended B-loop. Structural and kinetic data for APH(2'')-IIa, APH(2'')-IIIa and APH(2'')-IVa indicate that their spontaneous NTP hydrolysis is not regulated by this same mechanism owing to a significant structural rearrangement of the B-loop and the helical subdomain in these three enzymes. The observation that at least some APH phosphotransferases have a basal intrinsic NTPase activity indicates that while there is a price to pay for the bacteria to house these antibiotic-resistance enzymes, the ultimate benefit to the cell outweighs the wasteful energy loss. The evolution and the continued existence and proliferation of genes for the APH(2'') phosphotransferases in various bacterial species attests to this.

Acknowledgements

This work is based upon research conducted at the Stanford Synchrotron Radiation Lightsource (SSRL) at the SLAC National Accelerator Laboratory. Use of SSRL is supported by the DOE Office of Science, Office of Basic Energy Sciences under Contract No. DE-AC02-76SF00515 and also by the DOE Office of Science, Office of Workforce Development for Teachers and Scientists (WDTS) under the Science Undergraduate Laboratory Internships (SULI) Program (awarded to LM). The SSRL Structural Molecular Biology Program is supported by the DOE Office of Biological and Environmental Research and by the National Institutes of Health, National Institute of General Medical Sciences (including P41GM103393). The contents of this publication are solely the responsibility of the authors and do not necessarily represent the official views of NIGMS or NIH.

Funding information

This work was supported by grant 2R01AI057393 from the NIH/NIAID (to SBV).

References

- Adams, P. D., Afonine, P. V., Bunkóczi, G., Chen, V. B., Davis, I. W., Echols, N., Headd, J. J., Hung, L.-W., Kapral, G. J., Grosse-Kunstleve, R. W., McCoy, A. J., Moriarty, N. W., Oeffner, R., Read, R. J., Richardson, D. C., Richardson, J. S., Terwilliger, T. C. & Zwart, P. H. (2010). *Acta Cryst.* **D66**, 213–221.
- Badarau, A., Shi, Q., Chow, J. W., Zajicek, J., Mobashery, S. & Vakulenko, S. B. (2008). *J. Biol. Chem.* **283**, 7638–7647.
- Becker, B. & Cooper, M. A. (2013). *ACS Chem. Biol.* **8**, 105–115.
- Byrnes, L. J., Badarau, A., Vakulenko, S. B. & Smith, C. A. (2008). *Acta Cryst.* **F64**, 126–129.
- Caldwell, S. J., Huang, Y. & Berghuis, A. M. (2016). *Structure*, **24**, 935–945.
- Cantas, L., Shah, S. Q. A., Cavaco, L. M., Manaia, C. M., Walsh, F., Popowska, M., Garelick, H., Bürgmann, H. & Sørum, H. (2013). *Front. Microbiol.* **4**, 1–14.

- Carter, A. P., Clemons, W. M., Brodersen, D. E., Morgan-Warren, R. J., Wimberly, B. T. & Ramakrishnan, V. (2000). *Nature (London)*, **407**, 340–348.
- Chen, V. B., Arendall, W. B., Headd, J. J., Keedy, D. A., Immormino, R. M., Kapral, G. J., Murray, L. W., Richardson, J. S. & Richardson, D. C. (2010). *Acta Cryst.* **D66**, 12–21.
- Chen, Y., Mukherjee, S., Hoffmann, M., Kotewicz, M. L., Young, S., Abbott, J., Luo, Y., Davidson, M. K., Allard, M., McDermott, P. & Zhao, S. (2013). *Antimicrob. Agents Chemother.* **57**, 5398–5405.
- Davies, J. & Davies, D. (2010). *Microbiol. Mol. Biol. Rev.* **74**, 417–433.
- Davies, J. & Wright, G. D. (1997). *Trends Microbiol.* **5**, 234–240.
- De Pascale, G. & Wright, G. D. (2010). *ChemBioChem*, **11**, 1325–1334.
- Emsley, P., Lohkamp, B., Scott, W. G. & Cowtan, K. (2010). *Acta Cryst.* **D66**, 486–501.
- Endicott, J. A., Noble, M. E. & Johnson, L. N. (2012). *Annu. Rev. Biochem.* **81**, 587–613.
- Evans, P. R. & Murshudov, G. N. (2013). *Acta Cryst.* **D69**, 1204–1214.
- Fourmy, D., Recht, M. I., Blanchard, S. C. & Puglisi, J. D. (1996). *Science*, **274**, 1367–1371.
- Frase, H., Toth, M. & Vakulenko, S. B. (2012). *J. Biol. Chem.* **287**, 43262–43269.
- Gilbert, D. N. (2010). *Mandell, Douglas and Bennett's Principles and Practice of Infectious Diseases*, 7th ed., edited by G. L. Mandell, J. E. Bennett & R. Dolin, pp. 359–384. New York: Churchill Livingstone.
- Hon, W.-C., McKay, G. A., Thompson, P. R., Sweet, R. M., Yang, D. S. C., Wright, G. D. & Berghuis, A. M. (1997). *Cell*, **89**, 887–895.
- Johnson, L. N., Lowe, E. D., Noble, M. E. M. & Owen, D. J. (1998). *FEBS Lett.* **430**, 1–11.
- Johnson, L. N., Noble, M. E. M. & Owen, D. J. (1996). *Cell*, **85**, 149–158.
- Kabsch, W. (2010). *Acta Cryst.* **D66**, 125–132.
- Kaplan, E., Guichou, J.-F., Chaloin, L., Kunzelmann, S., Leban, N., Serpersu, E. H. & Lionne, C. (2016). *Biochim. Biophys. Acta*, **1860**, 802–813.
- Kim, C., Cha, J. Y., Yan, H., Vakulenko, S. B. & Mobashery, S. (2006). *J. Biol. Chem.* **281**, 6964–6969.
- Kim, C., Haddad, J., Vakulenko, S. B., Meroueh, S. O., Wu, Y., Yan, H. & Mobashery, S. (2004). *Biochemistry*, **43**, 2373–2383.
- Mahbub Alam, M., Kobayashi, N., Ishino, M., Sumi, A., Kobayashi, K., Uehara, N. & Watanabe, N. (2005). *Microb. Drug. Resistance*, **11**, 239–247.
- Majumder, K., Wei, L., Annedi, S. & Kotra, L. (2007). *Enzyme-Mediated Resistance to Antibiotics*, edited by R. Bonomo & M. Tolmasky, pp. 7–20. Washington, DC: ASM Press.
- Murshudov, G. N., Skubák, P., Lebedev, A. A., Pannu, N. S., Steiner, R. A., Nicholls, R. A., Winn, M. D., Long, F. & Vagin, A. A. (2011). *Acta Cryst.* **D67**, 355–367.
- Ngo, H. X. & Garneau-Tsodikova, S. (2016). *Structure*, **24**, 1011–1013.
- Ramirez, M. S. & Tolmasky, M. E. (2010). *Drug Resist. Updat.* **13**, 151–171.
- Setny, P. & Trylska, J. (2009). *J. Chem. Inf. Model.* **49**, 390–400.
- Shi, K. & Berghuis, A. M. (2012). *J. Biol. Chem.* **287**, 13094–13102.
- Shi, K., Houston, D. R. & Berghuis, A. M. (2011). *Biochemistry*, **50**, 6237–6244.
- Smith, C. A. & Baker, E. N. (2002). *Curr. Drug. Targets Infect. Dis.* **2**, 143–160.
- Smith, C. A., Toth, M., Bhattacharya, M., Frase, H. & Vakulenko, S. B. (2014). *Acta Cryst.* **D70**, 1561–1571.
- Smith, C. A., Toth, M., Frase, H., Byrnes, L. J. & Vakulenko, S. B. (2012). *J. Biol. Chem.* **287**, 12893–12903.
- Toth, M., Chow, J. W., Mobashery, S. & Vakulenko, S. B. (2009). *J. Biol. Chem.* **284**, 6690–6696.
- Toth, M., Frase, H., Antunes, N. T., Smith, C. A. & Vakulenko, S. B. (2010). *Protein Sci.* **19**, 1565–1576.
- Toth, M., Frase, H., Antunes, N. T. & Vakulenko, S. B. (2013). *Antimicrob. Agents Chemother.* **57**, 452–457.
- Vagin, A. & Teplyakov, A. (2010). *Acta Cryst.* **D66**, 22–25.
- Vicens, Q. & Westhof, E. (2003). *Biopolymers*, **70**, 42–57.
- Winn, M. D., Ballard, C. C., Cowtan, K. D., Dodson, E. J., Emsley, P., Evans, P. R., Keegan, R. M., Krissinel, E. B., Leslie, A. G. W., McCoy, A., McNicholas, S. J., Murshudov, G. N., Pannu, N. S., Potterton, E. A., Powell, H. R., Read, R. J., Vagin, A. & Wilson, K. S. (2011). *Acta Cryst.* **D67**, 235–242.
- Wright, G. D. (1999). *Curr. Opin. Microbiol.* **2**, 499–503.
- Wright, G. D. (2003). *Curr. Opin. Chem. Biol.* **7**, 563–569.
- Wright, G. D., Berghuis, A. M. & Mobashery, S. (1998). *Adv. Exp. Med. Biol.* **456**, 27–69.
- Young, P. G., Walanj, R., Lakshmi, V., Byrnes, L. J., Metcalf, P., Baker, E. N., Vakulenko, S. B. & Smith, C. A. (2009). *J. Bacteriol.* **191**, 4133–4143.